



Published in final edited form as:

Radiother Oncol. 2014 May ; 111(2): 281–288. doi:10.1016/j.radonc.2014.02.019.

Beam path toxicity in candidate organs–at-risk: Assessment of radiation emetogenesis for patients receiving head and neck intensity modulated radiotherapy

Esengul Kocak-Uzel, MD^{1,3}, G. Brandon Gunn, MD¹, Rivka R. Colen, MD¹, Micheal E Kantor, BS¹, Abdallah S R Mohamed, MD, MS^{1,4}, Sara Henley- Schoultz, BS⁵, Paniyotis Mavroidis, PhD⁶, Steven J. Frank, MD^{1,7}, Adam S. Garden, MD¹, Beth M. Beadle, MD, PhD¹, William H. Morrison, MD¹, Jack Phan, MD, PhD¹, David I. Rosenthal, MD¹, and Clifton D. Fuller, MD, PhD.^{1,7,*}

¹Department of Radiation Oncology, The University of Texas MD Anderson Cancer Center, Houston, Texas, USA

²Department of Radiology, The University of Texas MD Anderson Cancer Center, Houston, Texas, USA

³Department of Radiation Oncology, Sisli Etfal Teaching and Research Hospital, Istanbul, Turkey

⁴Department of Clinical Oncology, University of Alexandria, Alexandria, Egypt

⁵University of Texas Medical School at Houston, Houston, TX, USA

⁶Department of Radiation Oncology, The University of Texas Health Science Center at San Antonio, San Antonio, TX, USA

⁷The University of Texas Graduate School of Biomedical Sciences, Houston, TX, USA

Introduction

Intensity-modulated radiation therapy (IMRT) has become an increasingly common radiation treatment technique for head-and-neck (HN) cancers[1,2]. While 3D-conformal planning is used in many cases internationally[3], the dosimetric superiority of step-and-shoot IMRT[4,5], as well as potential further conformality gains in arc-based variants[6-8],

© 2014 Elsevier Ireland Ltd. All rights reserved.

*For correspondence and reprint requests contact: Clifton David Fuller, MD, PhD, The University of Texas MD Anderson Cancer Center, 1515 Holcombe Blvd., Unit 97, Houston, TX, 77030, Phone: 713-563-2334 Fax: 713-563-2366, cdfuller@mdanderson.org.

Conflict of Interest Notification: Dr. Fuller received/receives grant support from the following mechanisms: SWOG Hope Foundation Dr. Charles A. Coltman, Jr. Fellowship in Clinical Trials; the National Institutes of Health/National Cancer Institute Paul Calabresi Program in Clinical Oncology (K12CA088084-14) and Clinician Scientist Loan Repayment Program (L30 CA136381-02); Elekta AB/MD Anderson MR-LinAc Consortium Grant; GE Healthcare Technologies/MD Anderson Center for Advanced Biomedical Imaging In-Kind Award; Center for Radiation Oncology Research at MD Anderson Cancer Center Seed Grant; and the MD Anderson Institutional Research Grant Program. These listed funders/supporters played no role in the study design, collection, analysis, interpretation of data, manuscript writing, or decision to submit the report for publication.

Publisher's Disclaimer: This is a PDF file of an unedited manuscript that has been accepted for publication. As a service to our customers we are providing this early version of the manuscript. The manuscript will undergo copyediting, typesetting, and review of the resulting proof before it is published in its final citable form. Please note that during the production process errors may be discovered which could affect the content, and all legal disclaimers that apply to the journal pertain.

offers the advantage of improved tumor target coverage and critical normal tissue sparing[1], compared to 3D-conformal planning[9-11]. However, IMRT beam paths traverse normal tissues that may not have been directly irradiated in previous 2D and 3D techniques[2,12,13], resulting in distinct toxicity profiles from those seen in the pre-conformal radiotherapy era.

Among these symptom profiles are radiation-associated nausea and vomiting (RANV) symptoms. Radiotherapy alone to the head and neck region, in the pre-IMRT era, was held to have minimal risk of RANV[14,15], However, data suggest that is commonly encountered in radiation therapy for head and neck cancer patients. Even in the pre-*IMRT* era, an Italian prospective observational trial demonstrated that radiation-induced emesis occurred in 40% of head and neck patients treated with conventional radiation techniques[16]. Studies have demonstrated that field size, site of disease, and fractionation of radiation therapy are associated with RANV[17]. Compounding this is the degree to which concurrent chemotherapy, which can be highly emetogenic [18], may impact RANV.

Previously, our group presented a pilot evaluation of dosimetric parameters in patients receiving head and neck *IMRT* for a limited number of candidate structures[12] Building on our preliminary experience, we have investigated, in an expanded cohort, additional candidate organs-at-risk (OARs) as part of a larger effort to define candidate organ-at-risk constraints for beam path-attributable symptom reduction in patients receiving *IMRT* monotherapy.

The specific aims of the current study include:

- Interrogation of potential dose-response relationship between candidate emetogenesis-associated OARs and NV symptoms reported during intensity-modulated radiotherapy (*IMRT*) for chemotherapy-naive head and neck squamous cell carcinomas
- identification of OARs predominately associated with NV, for definitive *IMRT* and cohorts.
- assessment of literature reported candidate OAR constraints in a numerically robust dataset
- derivation of population-based dose-RANV thresholds CNV-ROIs for future validation for dose constraint/treatment plan selection
- generation of hypotheses for future prospective efforts.

Material and Methods

Patients Characteristics

A series of patients currently enrolled on a longitudinal patient reported outcome (PRO) assessment study were identified, and those treated with *IMRT* for squamous cell carcinomas of the head and neck between 2003 and 2013 were extracted from our institutional research database at our institution. Patient characteristics are summarized in Table 1. The original delivered DICOM-RT clinical treatment plan for each patient was

imported into a research database (Pinnacle 9.4, Phillips Medical Systems, Andover, MA). Planning CT DICOM files were exported into a commercial deformable registration/segmentation software[19] (Velocity AI 2.8.1, Velocity Medical Solutions, Atlanta, GA). For each patient, candidate emetogenesis-associated regions of interest (CNV-ROIs) (Figure 1, showing relevant CNV-ROIs; a representative anonymized case as both a DICOM and axial slices as a PDF file is included as a supplement file) were segmented manually by a single physician observer [XXX], with serial review by a faculty radiation oncologist [XXX] and a fellowship-trained attending neuroradiologist [XX]. Dose volume histograms (DVHs) were generated for each CNV-ROIs. Therefrom, delivered doses to these specific CNV-ROIs were reconstructed.

Clinical RANV data were reconstructed by review of records for all 130 patients. At each weekly visit during RT, nausea and vomiting are formally weekly assessed by nursing staff as standard practice. RANV events were defined as presence of any nursing-staff recorded nausea/emesis events between the start of IMRT and completion of therapy. Symptoms were evaluated before the start of IMRT and then at least once weekly during patient consultations by nursing assessment. To correlate NV toxicities with radiation doses to the newly added areas of interest, the number and frequency of vomiting episodes was extracted from the electronic nursing record (MOSAIQ, Elekta Medical Systems, Mountain Valley, CA) as CTC-AE (Common Toxicity Criteria for Adverse Events) version 4 vomiting scores recorded during the patient's weekly management visit while on treatment. Nausea was recorded in the treatment record as a binary variable (e.g. was subjective nausea experienced by the patient during the previous week during any week of IMRT). Nausea and vomiting reports were concatenated as a single composite binary "any NV" variable (e.g. was **any** subjective nausea and/or **any** CTC-AE vomiting event reported at **any time** during the course of therapy), and as a "CTC-V2+" variable (e.g. was vomiting rated as greater than CTC-AE grade 1, consisting of reported vomiting more than twice in a 24-hour period during **any** week of IMRT, and consistent with moderate-severe RANV).

Statistical evaluation

Statistical assessment was performed using JMP v 11Pro (SAS institute, Cary, NC). Mean dose to CNV-ROIs for those experiencing "any NV" or "CTC-V2+" were compared to those without symptoms using Wilcoxon rank test for each OAR, with Bonferroni correction for multiple comparisons. Logistic regression was performed using both "any NV" and "CTC-V2+ NV" with mean CNV-ROI dose as a continuous variable, to determine whether a dose-response effect might be observed, both for the entire cohort, likewise with Bonferroni correction.

In order to assess the relative contribution to RANV symptoms across multiple CNV-ROIs, and to derive exploratory non-model-dependent CNV-ROI dose-volume constraints recursive partitioning analysis (RPA) was performed. DVH data in 1 Gy bins for pooled CNV-ROIs was evaluated using RPA to allow identification and simultaneous dose-threshold selection all CNV-ROIs, using "Any N/V" as a discriminant. RPA allows selection of the "thresholds" for continuous variables using a binary categorization variable. RPA is especially suited to scenarios where it is desirable to select and "threshold"

continuous variable(s) associated with a categorical variable in the context of a multitude of predictor variables, even in the presence of complex interactions between candidate covariates[20]. Initially, a screen was performed within pooled DVH data for each CNV-ROIs using a bootstrap forest methodology to identify candidate thresholds for each OAR. Using “Any N/V” as a discriminator, for each of the 14 CNV-ROIs a bootstrap partition was undertaken using a forest of 100 trees after the first RPA split. The dominant column contributors were then selected for each CNV-ROI, and iterative partitions, with a minimum grouping of 20 patients per split/partition were performed until a split demonstrated a logworth value greater than the equivalent Bonferroni-corrected $p < 0.05$ (e.g. the 1st a priori split criteria was set at a $\logworth < 1.30/p < 0.05$, the 2nd split at $\logworth < 1.6/p < 0.025$, 3rd split $\logworth < 1.78/p < 0.016$, etc.), with pruning after non-significance, to distill candidate CNV-ROI thresholds for comparison with literature-derived CNV-ROI/OAR constraints.

Several previously literature-reported CNV-ROI constraint thresholds for NV symptoms were interrogated for association with “binary NV” and “CTC-V2+ NV” in our dataset, and compared to RPA-derived dose-constraint thresholds:

- mean brainstem dose of $>36\text{Gy}$ for brainstem [2].
- $V40 > 80\%$ for total vestibule [10].
- median dorsal vagus complex dose $> 26.9\text{Gy}$ [13].

Literature- and RPA-derived candidate CNV-ROI constraints were evaluated using univariate (Fisher’s exact test) and multivariate logistic regression for comparison in proportion of patients experiencing either toxicity variable(s).

Results

In total, 91 out of 130 (70%) patients receiving IMRT alone had recorded nausea/vomiting (“Any N/V”). Of these, 47 patients (36% of all IMRT patients) had CTC-AE v4 grade 2 or greater nausea/vomiting (“CTC-2+N/V”).

For all listed CNV-ROIs, mean dose to CNV-ROIs was uniformly lower for patients not experiencing RANV events (shown as boxplots in Figure 2), with varying degrees of statistical significance on Wilcoxon rank test analysis (Figure 3). Summary group DVH data by CNV-ROI is included as figures, showing a notable differential in dose profiles, especially in the 20-30Gy portions of the DVHs (Figures 4). Distributional analysis of CNV-ROIs dose the therapy cohort of Any N/V and CTC-2+N/V is summarized visually in Figure 3. Using “Any N/V” as a discriminator, a dose-response association was detectable for the area postrema and whole brain ROIs (both $p < 0.0015$), while for moderate/severe symptom cohorts a host of CNV-ROIs showed rank order differences (area postrema, brainstem, whole brain, medulla oblongata, oropharyngeal mucosa, dorsal vagus complex, and nucleus solitarius; all $p < 0.0007$), even with strict Bonferroni-corrected using Wilcoxon’s test p-value significance thresholds (Table 2 and Figure 3).

RPA analysis led to four RPA-derived candidate OAR dose-volume thresholds for univariate and multivariate assessment using “Any N/V” as a discriminant criteria: area

postrema V24 <76% (logworth 3.44; $p < 0.001$), whole brain V16 <5% (logworth 4.46; $p < 0.001$), oropharyngeal mucosa V70=0 (logworth 2.0, $p = 0.001$), nucleus solitaries V20 <99% (logworth 3.8; $p < 0.001$). Analysis of literature- and candidate RPA-derived OAR constraints revealed median DVC <26.9 Gy, and mean brainstem <36Gy, as well as the novel RPA-derived constraints of the area postrema, whole brain, and nucleus solitaries to be statistically significant on univariate assessment with Bonferroni-correction. On multiple comparison corrected multivariate analysis, only area postrema V24 <76% retained significance (Table 2).

Discussion

The recognition of beam path toxicities associated with *IMRT* in recent years has increased our awareness of the deleterious effects of incidental dose delivery to non-target OARs[2]. *IMRT* represents a potential shift in toxicity profiles due to technology implementation, as constrained dose to classic OAR drivers of toxicity (e.g. parotid dose reduction) may inadvertently result in low-dose bath deposition to previously unirradiated structure[2], a counterpoint to potential therapeutic gains[21].

In this study, delivered doses to fourteen structures were screened for dose-response effects with respect to binary RANV endpoints. Our data confirm a radiation dose-response relationship for several of these CNV-ROIs, namely the area postrema, brainstem, dorsal vagus complex, oropharyngeal mucosa, solitary nucleus and whole brain. Further, RANV appears associated with comparatively lower doses than traditional thresholds for tissue direct injury, as exemplified by the emergence of *area postrema V24* as a correlate of *IMRT*-associated emetogenesis.

For patients receiving *IMRT* alone, we observed a detectable dose-response for multiple structures. Furthermore, our data confirm the potential utility of both a literature-derived dose-response thresholds (*dorsal vagus complex median dose <26.9 Gy*[13]; *brainstem mean dose <36 Gy*[2]) and novel RPA-derived constraints (*area postrema V24 <76%*). These dose-constraint thresholds suggest that even comparatively low-dose “bath” to CNS structures can be associated with demonstrable symptom burden, an observation supported by comparison of pooled DVH data (Figure 4), wherein percent-volume CNV-ROIs for those experiencing RANV events is most distinct in the 20-40 Gy range, rather than higher dose regions. The difference in pooled DVH data is even more pronounced when moderate/severe (e.g. CTC-V2+) nausea and vomiting is considered, as illustrated visually by non-overlapping 95% CI bars seen in both Figure 4 and Supplementary Figure 1 [22]. Importantly, these doses are far below those associated with neuropathy and/or necrosis in standard dose-toxicity models [23].

The current study utilized non-model-dependent RPA analysis, which circumvents the fact that for many of the investigated CNV-ROI structures, limited radiobiologic model data exists regarding dose dependent toxicities. Likewise, RPA has methodologic advantages for screening thresholds related to toxicity, as several CNV-ROIs are subvolumes of other screened CNV-ROIs (e.g. the dorsal vagus complex and area postrema are fully

encapsulated within the brainstem). However, efforts are underway to use the current dataset using established radiobiologic modeling methods[24-27].

The CNV-ROIs used for the current study have only recently been investigated for fractionated head and neck *IMRT*[12,28], though some have been associated with RANV in hypofractionated CNS radiotherapy for some time[29,30]. The area postrema, dorsal vagal complex, and vestibules have been identified as CNV-ROIs of interest in previous studies [12,31,32]. Previously, our group demonstrated mean and median brainstem doses consistently <5Gy delivered using classic conventional (non-conformal) techniques, with minimal NV reporting. In comparison, mean doses of 25-35Gy to the brainstem were observed for patients using *IMRT* techniques, with a statistically significant increase in NV reporting[2]. A previous retrospective study of 100 patients with oropharyngeal cancer treated with *IMRT*, with and without chemotherapy, failed to show a dose-response to brainstem, AP and DVC with Bonferroni correction application; however, given the number of statistical comparisons, we sought in the current study to include sufficient numbers of patients treated with a homogenous step-and shoot *IMRT* treatment paradigm, without concurrent nor induction chemotherapy (n=130) to allow robust comparison of multiple CNV-ROIs confounding effects of chemotherapy.

A prospective study of 49 patients with nasopharyngeal carcinoma (NPC) treated with *IMRT* published by Lee *et al.* also failed to demonstrate that the dose to brainstem, area postrema and dorsal vagus complex, correlated with NV, instead proposing the vestibules as a CNV-ROI in radiation-induced NV, specifically a V40 of the total vestibules. While our dataset had comparatively few NPC cases total vestibule V40>80% did not emerge on univariate nor multivariate analysis as a significant correlate of RANV [28]. Similarly, a study of 43 patients with various types of head and neck cancers by Monroe *et al.* indicated that the dose to the DVC (which consists of the AP together with the nucleus solitarius and dorsal motor nucleus of the vagus) was related to RANV. In our more numerically powerful dataset, median dose DVC >26.9 Gy, as proposed by Monroe *et al.* and mean brainstem dose as Rosenthal *et al.* suggested, were indeed found significant in univariate analysis, but failed to reach significance on multivariate assessment [13].

Our data point to potential for clinically significant modification of a common therapy-associated sequelae through reduction in low- and intermediate-dose delivery to specified OARs. Conceivably, technical modification (such as improved delivery via arc-based methods[33] or proton radiotherapy[34,35]), and thus represents a feasible clinical aim of technology development if dose to target volumes is not in any manner compromised. Future studies should assess the capacity to spare low- and intermediate-dose bath to CNS structures adjacent to the head and neck as part of a comprehensive toxicity minimization strategy.

The current series has several notable limitations. As a retrospective single-institution dataset, the standard caveats apply. While extreme effort was made to ensure reliability of CNV-ROI segmentation by neuroradiologist oversight, OAR delineation is always subject to observer error[36]. The majority of our patients had oropharyngeal disease, yet inclusion of other head and neck sites, as well as the heterogeneity of therapies employed results in

potential clinical confounders.. Additionally, investigation of multiple spatially adjacent CNV-ROIs for dose-response effects resulted in multiple comparisons requiring statistical correction, and thus must be validated before direct clinical implementation at other facilities.

Nonetheless, our data represents by far the numerically largest extant reported investigation of organs-at-risk dose-response for nausea and vomiting in head and neck *IMRT*. Our data confirms dose-response associations for several central nervous system structures in patients receiving *IMRT* alone for head and neck cancers, and provides benchmark data for future investigations.

In conclusion, RANV is a common therapy-related morbidity facing patients receiving definitive head and neck *IMRT*, and is associated with increased dose to specific CNS structures. Future efforts to develop technical and pharmacologic interventions to reduce RANV are an important future area of research. More granular models of dose-response are desirable and are a targeted research aim for future studies. When possible, dose to relevant CNV-ROIs (such as the area postrema) should be routinely monitored and constrained when feasible given adequate tumor coverage, even for low/intermediate doses unlikely to cause necrosis or neuropathy.

Supplementary Material

Refer to Web version on PubMed Central for supplementary material.

References

1. Nutting CM, Morden JP, Harrington KJ, et al. Parotid-sparing intensity modulated versus conventional radiotherapy in head and neck cancer (PARSPORT): a phase 3 multicentre randomised controlled trial. *The lancet oncology*. 2011; 12:127–136. [PubMed: 21236730]
2. Rosenthal DI, Chambers MS, Fuller CD, et al. Beam path toxicities to non-target structures during intensity-modulated radiation therapy for head and neck cancer. *International journal of radiation oncology, biology, physics*. 2008; 72:747–755.
3. Herrassi MY, Bentayeb F, Malisan MR. Comparative study of four advanced 3d-conformal radiation therapy treatment planning techniques for head and neck cancer. *J Med Phys*. 2013; 38:98–105. [PubMed: 23776314]
4. Cilla S, Deodato F, Digesu C, et al. Assessing the feasibility of volumetric-modulated arc therapy using simultaneous integrated boost (SIB-VMAT): An analysis for complex head-neck, high-risk prostate and rectal cancer cases. *Med Dosim*. 2014; 39:108–116. [PubMed: 24342167]
5. Al-Mamgani A, Van Rooij P, Tans L, Teguh DN, Levendag PC. Toxicity and outcome of intensity-modulated radiotherapy versus 3-dimensional conformal radiotherapy for oropharyngeal cancer: a matched-pair analysis. *Technology in cancer research & treatment*. 2013; 12:123–130. [PubMed: 23098281]
6. Holt A, Van Gestel D, Arends MP, et al. Multi-institutional comparison of volumetric modulated arc therapy vs. intensity-modulated radiation therapy for head-and-neck cancer: a planning study. *Radiat Oncol*. 2013; 8:26. [PubMed: 23369221]
7. Van Gestel D, van Vliet-Vroegindewij C, Van den Heuvel F, et al. RapidArc, SmartArc and TomoHD compared with classical step and shoot and sliding window intensity modulated radiotherapy in an oropharyngeal cancer treatment plan comparison. *Radiat Oncol*. 2013; 8:37. [PubMed: 23425449]

8. Uzel EK, Karacam S, Elicin O, Uzel O. Comparison of two different IMRT planning techniques in the treatment of nasopharyngeal carcinoma. Effect on parotid gland radiation doses. *Strahlenther Onkol.* 2013; 189:552–558. [PubMed: 23748231]
9. Wolden SL, Chen WC, Pfister DG, Kraus DH, Berry SL, Zelefsky MJ. Intensity-modulated radiation therapy (IMRT) for nasopharynx cancer: update of the Memorial Sloan-Kettering experience. *International journal of radiation oncology, biology, physics.* 2006; 64:57–62.
10. Lee N, Harris J, Garden AS, et al. Intensity-modulated radiation therapy with or without chemotherapy for nasopharyngeal carcinoma: radiation therapy oncology group phase II trial 0225. *Journal of clinical oncology : official journal of the American Society of Clinical Oncology.* 2009; 27:3684–3690. [PubMed: 19564532]
11. Kam MK, Teo PM, Chau RM, et al. Treatment of nasopharyngeal carcinoma with intensity-modulated radiotherapy: the Hong Kong experience. *International journal of radiation oncology, biology, physics.* 2004; 60:1440–1450.
12. Ciura K, McBurney M, Nguyen B, et al. Effect of brain stem and dorsal vagus complex dosimetry on nausea and vomiting in head and neck intensity-modulated radiation therapy. *Medical dosimetry : official journal of the American Association of Medical Dosimetrists.* 2011; 36:41–45. [PubMed: 20097059]
13. Monroe AT, Reddy SC, Gibbs GL, White GA, Peddada AV. Factors associated with radiation-induced nausea and vomiting in head and neck cancer patients treated with intensity modulated radiation therapy. *Radiotherapy and oncology : journal of the European Society for Therapeutic Radiology and Oncology.* 2008; 87:188–194. [PubMed: 18237801]
14. Feyer PC, Maranzano E, Molassiotis A, Roila F, Clark-Snow RA, Jordan K. Radiotherapy-induced nausea and vomiting (RINV): MASCC/ESMO guideline for antiemetics in radiotherapy: update 2009. *Supportive care in cancer : official journal of the Multinational Association of Supportive Care in Cancer.* 2011; 19(Suppl 1):S5–14. [PubMed: 20697746]
15. Feyer P, Maranzano E, Molassiotis A, et al. Radiotherapy-induced nausea and vomiting (RINV): antiemetic guidelines. *Supportive care in cancer : official journal of the Multinational Association of Supportive Care in Cancer.* 2005; 13:122–128. [PubMed: 15592688]
16. The Italian Group for Antiemetic Research in Radiotherapy. Radiation-induced emesis: a prospective observational multicenter Italian trial. *International journal of radiation oncology, biology, physics.* 1999; 44:619–625.
17. Urba S. Radiation-induced nausea and vomiting. *Journal of the National Comprehensive Cancer Network : JNCCN.* 2007; 5:60–65. [PubMed: 17239327]
18. Fraunholz I, Grau K, Weiss C, Rodel C. Patient- and treatment-related risk factors for nausea and emesis during concurrent chemoradiotherapy. *Strahlenther Onkol.* 2011; 187:1–6. [PubMed: 21234525]
19. Kirby N, Chuang C, Ueda U, Pouliot J. The need for application-based adaptation of deformable image registration. *Med Phys.* 2013; 40:011702. [PubMed: 23298072]
20. Strobl C, Malley J, Tutz G. An introduction to recursive partitioning: rationale, application, and characteristics of classification and regression trees, bagging, and random forests. *Psychol Methods.* 2009; 14:323–348. [PubMed: 19968396]
21. Beadle BM, Liao KP, Elting LS, et al. Improved survival using intensity-modulated radiation therapy in head and neck cancers: A SEER-Medicare analysis. *Cancer.* 2014
22. Cumming G, Fidler F, Vaux DL. Error bars in experimental biology. *J Cell Biol.* 2007; 177:7–11. [PubMed: 17420288]
23. Mayo C, Yorke E, Merchant TE. Radiation associated brainstem injury. *International journal of radiation oncology, biology, physics.* 2010; 76:S36–41.
24. Mavroidis P, Lind BK, Theodorou K, et al. Statistical methods for clinical verification of dose-response parameters related to esophageal stricture and AVM obliteration from radiotherapy. *Phys Med Biol.* 2004; 49:3797–3816. [PubMed: 15446806]
25. Su FC, Mavroidis P, Shi C, Ferreira BC, Papanikolaou N. A graphic user interface toolkit for specification, report and comparison of dose-response relations and treatment plans using the biologically effective uniform dose. *Comput Methods Programs Biomed.* 2010; 100:69–78. [PubMed: 20338661]

26. Mavroidis P, Ferreira BC, Lopes Mdo C. Response-probability volume histograms and iso-probability of response charts in treatment plan evaluation. *Med Phys.* 2011; 38:2382–2397. [PubMed: 21776773]
27. Roland T, Tryggestad E, Mavroidis P, Hales R, Papanikolaou N. The radiobiological P(+) index for pretreatment plan assessment with emphasis on four-dimensional radiotherapy modalities. *Med Phys.* 2012; 39:6420–6430. [PubMed: 23039677]
28. Lee VH, Ng SC, Leung TW, Au GK, Kwong DL. Dosimetric predictors of radiation-induced acute nausea and vomiting in IMRT for nasopharyngeal cancer. *International journal of radiation oncology, biology, physics.* 2012; 84:176–182.
29. Alexander E 3rd, Siddon RL, Loeffler JS. The acute onset of nausea and vomiting following stereotactic radiosurgery: correlation with total dose to area postrema. *Surg Neurol.* 1989; 32:40–44. [PubMed: 2660309]
30. Bodis S, Alexander E 3rd, Kooy H, Loeffler JS. The prevention of radiosurgery-induced nausea and vomiting by ondansetron: evidence of a direct effect on the central nervous system chemoreceptor trigger zone. *Surg Neurol.* 1994; 42:249–252. [PubMed: 7940114]
31. Eisbruch A, Ten Haken RK, Kim HM, Marsh LH, Ship JA. Dose, volume, and function relationships in parotid salivary glands following conformal and intensity-modulated irradiation of head and neck cancer. *International journal of radiation oncology, biology, physics.* 1999; 45:577–587.
32. Miller AD, Leslie RA. The area postrema and vomiting. *Frontiers in neuroendocrinology.* 1994; 15:301–320. [PubMed: 7895890]
33. Vanetti E, Clivio A, Nicolini G, et al. Volumetric modulated arc radiotherapy for carcinomas of the oro-pharynx, hypo-pharynx and larynx: a treatment planning comparison with fixed field IMRT. *Radiotherapy and oncology : journal of the European Society for Therapeutic Radiology and Oncology.* 2009; 92:111–117. [PubMed: 19157609]
34. Kandula S, Zhu X, Garden AS, et al. Spot-scanning beam proton therapy vs intensity-modulated radiation therapy for ipsilateral head and neck malignancies: a treatment planning comparison. *Med Dosim.* 2013; 38:390–394. [PubMed: 23916884]
35. Simone CB 2nd, Ly D, Dan TD, et al. Comparison of intensity-modulated radiotherapy, adaptive radiotherapy, proton radiotherapy, and adaptive proton radiotherapy for treatment of locally advanced head and neck cancer. *Radiotherapy and oncology : journal of the European Society for Therapeutic Radiology and Oncology.* 2011; 101:376–382. [PubMed: 21663988]
36. Mukesh M, Benson R, Jena R, et al. Interobserver variation in clinical target volume and organs at risk segmentation in post-parotidectomy radiotherapy: can segmentation protocols help? *Br J Radiol.* 2012; 85:e530–536. [PubMed: 22815423]

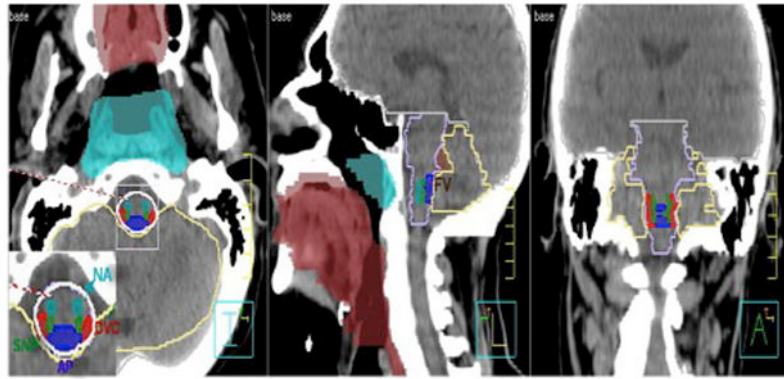


Figure 1. Sagittal, coronal, axial view of the CNV-ROIs: DVC (Dorsal vagal complex), AP (Area postrema), NA (Nucleus ambiguus) SN (Solitary Nucleus), BS (Brainstem), FV (Fourth Ventricle), NF (Nasopharyngeal mucosa), Cerebellum, Mucosa (Oropharyngeal mucosa), Pons (Pons), WB (Whole brain)



Figure 2. Distribution boxplots of mean dose for all ROIs, showing OAR-dose for those patients experiencing **any** RANV (“Any N/V”), or >moderate/severe RANV (“CTC-V2+”, none reported or reported during therapy), color coded by Wilcoxon test significance level for all listed CNV-ROIs. Red boxplot pairs show failure to meet $p < 0.05$ threshold, while green boxplot pairs indicate statistical significance under strict multiple-comparison correction ($0.05/28$, or $p < 0.0018$). for each of the 28 comparisons (i.e. 14 CNV-ROIs for each of 2 toxicity cohorts). Notably, in all cases, for all ROIs, cumulative grand mean doses were higher for those patients experiencing RANVs. DVC (Dorsal vagal complex), AP (Area postrema), NA (Nucleus ambiguus) SN (Solitary Nucleus), BS (Brainstem), FV (Fourth Ventricle), NF (Nasopharyngeal mucosa), Cer (Cerebellum), Muc (Oropharyngeal mucosa), Pon (Pons), WB (Whole brain)

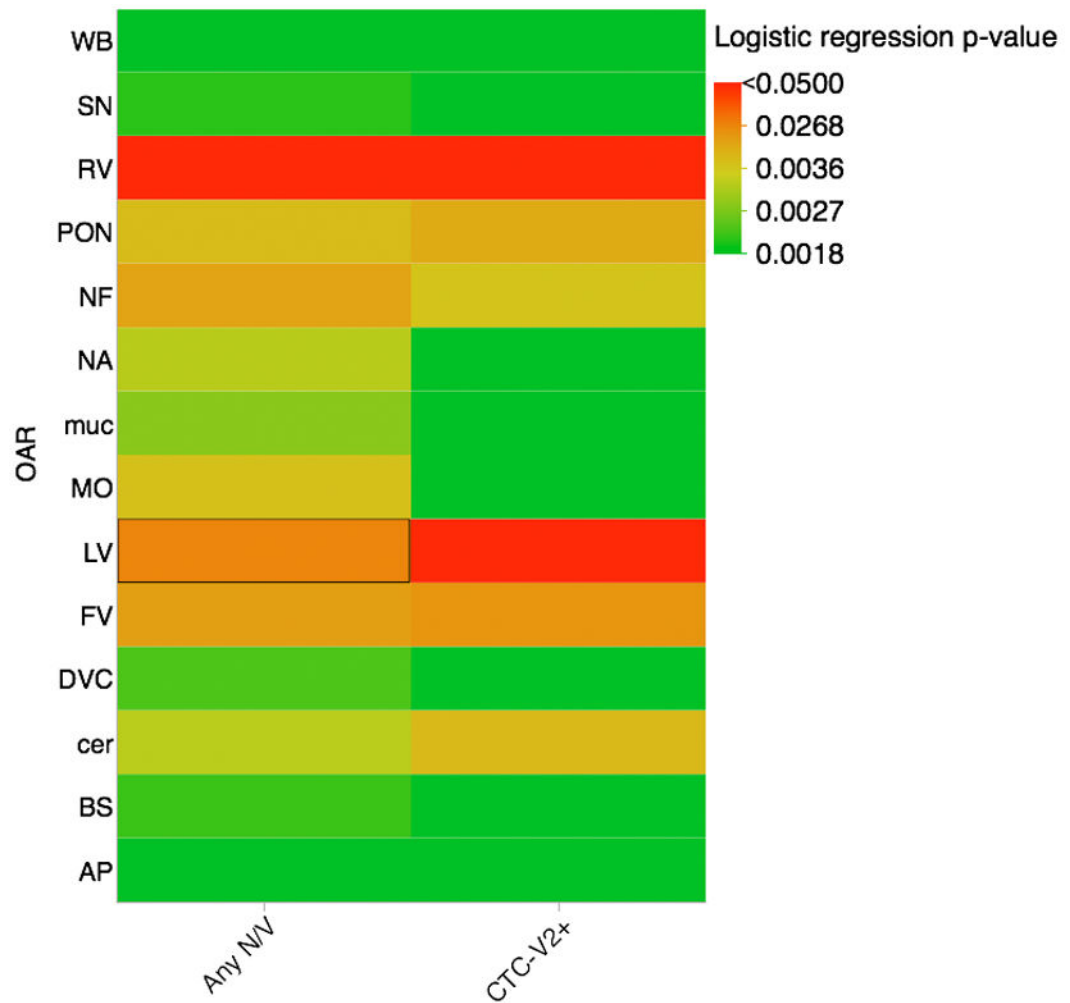


Figure 3. Heatmap of statistical significance for utilized analyses; allowing visual representation of Bonferroni correction. Solid red squares denote lack of statistical significance at even the grossest level ($p > 0.05$), while solid green squares indicate statistical significance under strict multiple-comparison correction ($0.05/28$, or $p < 0.0018$). for each of the 28 comparisons (i.e. 14 CNV-ROIs for each of 2 toxicity cohorts).

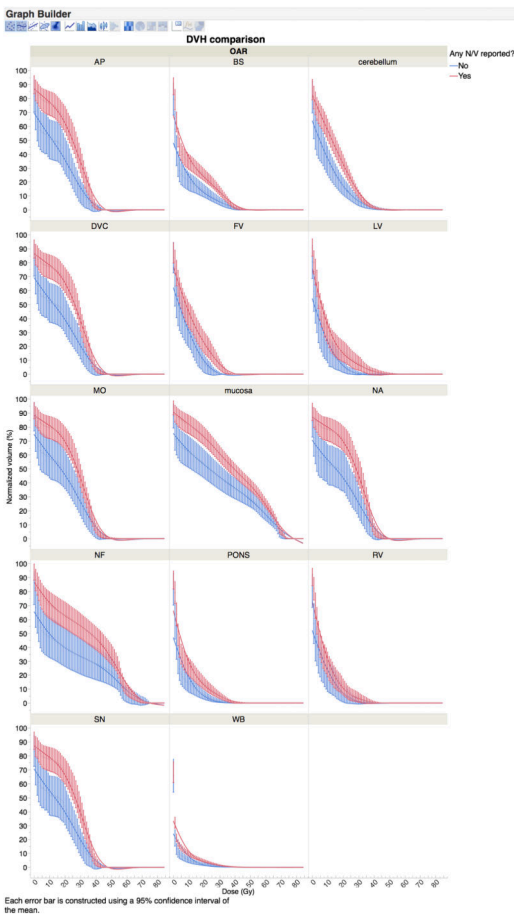


Figure 4. (Any NV): Plot of mean (thick line) and 95% mean confidence interval (bars) for cumulative DVHs of patients experiencing any nausea/vomiting events during therapy (red) compared to those without said symptoms (blue), with DVH binned in 1-Gy increments. Broadly, if 95% confidence intervals do not overlap mean lines, for each bin there is a difference at the $p < 0.05$ level; if error bars do not overlap entirely overlap, the p-value is < 0.01 for the specified 1-Gy dose bin without multiple comparison correction. DVC (Dorsal vagal complex), AP (Area postrema), NA (Nucleus ambiguus) SN (Solitary Nucleus), BS (Brainstem), FV (Forth Ventricle), NF (Nasopharyngeal mucosa), Cerebellum, Mucosa (Oropharyngeal mucosa), Pons (Pons), WB (Whole brain)

Table 1

Patients Characteristics

Age (years)	
Range	35-83
Median	59
Sex (no. pts)	
Male	98 (75%)
Female	32 (25%)
T Stage (no. pts)	
T1	63(48%)
T2	49(38%)
T3	7 (5%)
T4	2 (2%)
Tx	9 (7%)
N Stage (no. pts)	
N0	33 (25%)
N1	35 (27%)
N2	47 (36%)
N3	4 (3%)
Nx	11 (8%)
Primary sites (no. pts)	
Base of Tongue	17 (13%)
Tonsil	88 (68%)
Larynx/Nasopharyngeal/Maxillary sinus	25 (19%)
Symptom cohorts (no. pts/percent)	
No nausea/vomiting reported	39 (30%)
Any N/V reported	91 (70%)
CTC-V2+ reported	47 (36%)

Table 2

Four RPA-derived candidate OAR-dose-thresholds for univariate and multivariate assessment using comparison of p-values.

Source	MV	UV
DVC median \geq 26.9%	0.054121932	0.0014*
BS Mean \geq 36Gy	0.08	0.0022*
TV 40>80%	0.548212802	0.3504
Mucosa V70 >0	0.081683735	0.0055
AP V24 \geq 76%	0.021464091*	0.0001*
WB V16 >5%	0.044658738	0.0001*
SN V20>99%	0.417539352	0.0001*